Origins and Mechanisms of Eastern Pacific Tropical Cyclogenesis: A Case Study

JOHN MOLINARI, DAVID VOLLARO, STEVEN SKUBIS, AND MICHAEL DICKINSON

Department of Earth and Atmospheric Sciences, University at Albany, State University of New York, Albany, New York

(Manuscript received 26 June 1998, in final form 7 January 1999)

ABSTRACT

The genesis of Hurricane Hernan (1996) in the eastern Pacific was investigated using gridded analyses from the European Centre for Medium-Range Weather Forecasts and gridded outgoing longwave radiation. Hernan developed in association with a wave in the easterlies that could be tracked back to Africa in longitude–time plots of the filtered v component of the wind (2–6-day period) at 700 mb. The wave crossed Central America near Lake Nicaragua with little change in its southwest–northeast tilt, but the most intense convection shifted from near the wave axis in the Caribbean to west of the wave axis in the Pacific. The wave intensified as it moved through a barotropically unstable background state (defined by a low-pass filter with a 20-day cutoff) in the western Caribbean and eastern Pacific. A surge in the southwesterly monsoons and enhanced convection along 10°N occurred to the west of the 700-mb wave in the Pacific and traveled with the wave. This had the effect of enhancing low-level vorticity over a wide region ahead of the 700-mb wave. Available evidence suggests that additional low-level vorticity was produced by enhanced flow from the north through the Isthmus of Tehuantepec as the 700-mb wave approached. Depression formation did not occur until 6–12 h after the 700-mb wave reached this region of large low-level vorticity in the Gulf of Tehuantepec.

Eastern Pacific SST and vertical wind shear magnitude are typically favorable for tropical cyclone development in Northern Hemisphere summer and early fall. Because the favorable mountain interaction and the surge in the low-level monsoons appear to relate directly to the wave in the easterlies, it is argued that the strength of such waves reaching Central America from the east is the single most important factor in whether subsequent eastern Pacific cyclogenesis occurs. Possible parallels with western Pacific cyclogenesis are discussed.

1. Introduction

Tropical cyclogenesis remains poorly understood. Riehl (1954) stated ''we observe universally that tropical storms form only within preexisting disturbances.'' In a review of the topic, McBride (1995) noted that such disturbances can be seen via satellite as ''cloud clusters,'' convectively active disturbances of a scale comparable to that of the outer envelope of a mature tropical cyclone, but much larger in scale than the tropical cyclone core. The cloud clusters develop within synoptic-scale cyclonic disturbances such as a monsoon trough or a wave in the easterlies. In turn the synoptic-scale disturbances, and possibly the cloud clusters as well, appear to be influenced by even larger scales (Liebmann et al. 1994; Molinari et al. 1997) such as the Madden–Julian oscillation (MJO; Madden and Julian 1994). Observational studies repeatedly show the enormous control that various larger-scale circulations have on whether tropical cyclones will form.

Much debate has occurred of late (e.g., Smith 1997) over the merits and interpretations of the two formal theories of tropical cyclogenesis, conditional instability of the second kind (CISK; Charney and Eliassen 1964; Ooyama 1964) and wind-induced surface heat exchange (WISHE; Emanuel 1986; Emanuel et al. 1994). Whatever the relative merits of these theories, including their conceptual value at the mature stage (Ooyama 1982), it can be said without ambiguity that neither includes any realistic representation of the influence of synoptic and planetary-scale circulations on tropical cyclogenesis. Nor do they incorporate the azimuthally asymmetric evolution of incipient tropical cyclones. Rather, they appear most relevant once a nearly symmetric low-level circulation has been established, at which time large-scale controls may have less influence and axisymmetric processes may dominate the inner-core evolution. Because such theories cannot address the earlier transition from cloud cluster or wave to depression, observational and numerical studies must be relied on at present.

In terms of genesis events per unit area and per unit time, the eastern Pacific Ocean is the most active tropical cyclone formation region on earth. As such it provides a useful basin for investigating the role of larger-scale influences on tropical cyclogenesis. In the current paper, the genesis of a single eastern Pacific storm, Hurricane

Corresponding author address: Dr. John Molinari, Department of Earth and Atmospheric Sciences, University at Albany, State Univeristy of New York, 1400 Washington Ave., Albany, NY 12222.
E-mail: molinari@atmos.albany.edu

Hernan of 1996, will be examined. An attempt will be made to put the results into an integrated framework for understanding eastern Pacific tropical cyclogenesis.

2. Methodology

Merrill (1984) noted the confusion of terminology when referring to formation and intensification of tropical cyclones. For the purposes of this paper, *genesis* will refer to the development of a tropical depression from a preexisting disturbance, following Frank (1987). Because the definition of a depression requires closed isobars at the surface, the tightly coupled connection between a tropical cyclone and the underlying ocean may be said to begin at that time. In addition, large-scale influences appear to have much greater impact on whether a depression initially develops than whether an existing depression intensifies further (Liebmann et al. 1994). As a result, evaluating the role of large-scale circulations would seem most appropriate at the time just before a tropical depression develops. Of course, operational estimates of this time are only approximate, but the error in timing is likely to be much less than the 12-h separation of large-scale analyses used in this study.

Molinari et al. (1997) used potential vorticity (hereafter PV) as a key variable in their analysis. In the current study, the shallow monsoonal flow in the eastern Pacific is a critical component. It is difficult to calculate meaningful values of Ertel PV on isentropic surfaces close to the surface owing to difficulties with the vertical derivative $\partial p/\partial\theta$. In addition, the presence of mountains that are strongly heated creates diurnal fluctuations in PV. Pressure-surface analyses and absolute vorticity will substitute in this paper for the isentropic analyses and PV of the previous paper.

Low-pass and bandpass time filters follow the methods described by Molinari et al. (1997). The low-pass filter has a cutoff of 20 days, and will be interpreted as the slowly varying background state. The 2–6-day bandpass filter will be interpreted as the easterly wave scale.

Outgoing longwave radiation (OLR) data follow the procedures of Gruber and Winston (1978), but using the improved interpolation for missing data by Liebmann and Smith (1996). These data are available on a 2.5° lat $\times$ 2.5° long grid.

All results in this paper other than those showing OLR come from calculations using 1.125° lat $\times$ 1.125° long gridded analyses from the European Centre for Medium-Range Weather Forecasts (ECMWF). Many supporting arguments for the value of ECMWF analyses in studying the environment of hurricanes have been given in previous papers (Molinari and Vollaro 1990; Molinari et al. 1992, 1995, 1997), and the results of those papers provide further support. The value of such analyses will be reexamined here because the eastern Pacific is especially data sparse, and because the genesis of a specific hurricane is being studied.

ECMWF gridded analyses have been used extensively to study both synoptic- and planetary-scale tropical waves (e.g., Nitta and Takayabu 1985; Reed et al. 1988a,b; Liebmann and Hendon 1990; Lau and Lau 1990). These studies have shown that the analyzed waves have remarkable consistency with independently derived fields such as OLR or other satellite-derived products, even over tropical oceans where conventional data are lacking (Liebmann and Hendon 1990; Reed et al. 1988a,b). In general, where data exist, the ECMWF analyses are successful in incorporating them. Where data are absent, no ground truth exists to evaluate the analyses. In such regions the four-dimensional analysis/assimilation (Lorenc 1981) essentially fills in with a ''full-physics'' numerical simulation constrained by 6-hourly injection of data from surrounding regions. This appears to be the best alternative available at present. Recently M. Wheeler (1998, personal communication) noted that dynamical fields from the National Centers for Environmental Prediction reanalysis contain tropical waves whose spectral characteristics match reasonably well those determined from OLR alone by Wheeler and Kiladis (1999). A general circulation model, on the other hand, did not contain a realistic representation of such tropical waves (M. Wheeler 1998, personal communication). It appears that even sparse unevenly spaced data contribute greatly to the realistic depiction of tropical waves and disturbances in operational global analyses.

Nevertheless, the timing and location of tropical depression formation in the eastern Pacific are often not well represented by the ECMWF analyses. This reflects the combination of a lack of data and the inability of the global model (and thus the data assimilation cycle) to spin up tropical depressionlike vortices where no data support their existence. As a result, before pursuing a particular case study the performance of the analysis must be examined fully.

Hurricane Hernan (1996) in the eastern Pacific was chosen for this study. Forecasters at the National Hurricane Center (now known as the Tropical Prediction Center; R. Pasch and L. Avila 1997, personal communication) identified the pre-Hernan disturbance as relatively easy to track from Africa to the eastern Pacific, and identified September 1996 as having well-defined waves. The veracity of the analyses was evaluated in three steps. First, sequences of 12-hourly analyses in the days prior to the development of the tropical depression that ultimately became Hurricane Hernan were examined at several levels in the vertical for ''time continuity.'' Although this is a subjective measure, it is tied to meaningful physical constraints such as quasi-conservation of PV. It will be shown (Fig. 5) that a well-defined, slowly varying disturbance in the easterlies at 700 mb propagates westward over several days.

Second, the observed position and timing (using ''best-track'' data) of the first appearance of the pre-Hernan tropical depression were compared to the ana-

lyzed fields. The tropical depression formed at 0600 UTC 30 September at 12.6°N, 98.7°W; Hernan was named a tropical storm at 1800 UTC 30 September at 12.9°N, 100.7°W. The gridded analyses are at 0000 and 1200 UTC times. As will be seen in Fig. 6, a strong surface vortex (15.7 m s^{-1} maximum wind) first appeared in the gridded analyses at 0000 UTC 30 August, and reached tropical storm strength (21 m s^{-1}) at 0000 UTC 1 October. Figure 6, taking into account the 6-h time differences, will show that the location of the pre-Hernan disturbance was also well represented by the analyses.

Finally, the evolution shown in the analyses was compared to independent data. It will be seen that OLR fields provide support for the structure and evolution of the pre-Hernan disturbance in the ECMWF analyses.

Because the analyses meet the time continuity, tropical depression timing and location, and OLR consistency criteria, it has been assumed they are sufficiently accurate for further study. Nevertheless, as noted by Molinari et al. (1997), detailed quantitative calculations of relatively high-frequency disturbances (i.e., periods less than 6 days) must be approached with caution. In this paper the more qualitative aspects of such disturbances (position and structure rather than, e.g., calculations of energy exchanges) will be examined. In addition, only the behavior of the preexisting synoptic-scale disturbance up to the time of depression formation will be examined. It is concluded that the ECMWF analyses can be of considerable value, but must be treated with appropriate caution and skepticism in regions without extensive data.

3. Previous studies of tropical cyclogenesis

a. Role of monsoon troughs

Gray (1968) described a set of necessary conditions for tropical cyclogenesis that likely apply in all regions. In a review of the topic, McBride (1995) describes a number of mechanisms that, although they were proposed for the western Pacific or Australian region, could be relevant to the eastern Pacific, because all three basins contain a monsoon trough. McBride and Zehr (1981) found enhanced relative vorticity in the lower troposphere on a 1000–2000-km scale in the environment of cloud clusters that developed into tropical cyclones, compared to nondeveloping clusters. Love (1985) described ''surges'' in the westerly winds south of the monsoon trough associated with cold outbreaks from the winter hemisphere. This was hypothesized to come about via accelerating flow into the monsoon trough as a result of the increased magnitude of the latitudinal pressure gradient at the surface. Often the subtropical ridge poleward of the monsoon trough simultaneously intensified (the reasons are unclear), creating stronger easterlies to the north of the monsoon trough as well. Davidson and Hendon (1989) found a similar evolution in the Australian monsoon. The result in both cases was much greater vorticity within the monsoon trough before genesis, consistent with the findings of McBride and Zehr (1981).

Holland (1995) showed the results of a simulation of monsoonal flow with a three-dimensional model. By specifying a Gaussian distribution in x and y of diabatic heating over a relatively small region, Holland (1995) was able to simulate many aspects of the western Pacific monsoon at 850 mb, including the subtropical ridge to the north and the ridge just south of the equator. Holland attributed the ridges to Rossby wave dispersion. Holland's result offers a plausible reason, enhanced convective heating in the monsoon trough, for both the stronger trough and the stronger ridge to the north found by Love (1985). Holland speculated that middle latitude interactions, such as the southward movement of a frontal zone, could trigger the enhanced convection.

Holland (1995) speculated that easterly waves could grow in the western Pacific where trade wind easterlies met monsoon westerlies via Rossby wave accumulation, essentially convergence of the group velocity. This region is known to be favored for development of depressions (Briegel and Frank 1997). Sobel and Bretherton (1998) provided evidence that the easterly waves behaved like nondivergent Rossby waves, and carried out calculations that support the wave accumulation argument in the western Pacific.

Zehr (1992) presented a schematic diagram of tropical cyclogenesis in the western Pacific that contained elements of more than one of the above hypotheses. Zehr's schematic showed a disturbance in the easterlies approaching the longitude of the monsoon westerlies. Also part of the schematic was a surge in the monsoons about one-half wavelength ahead (west) of the easterly wave. Zehr's schematic thus includes an easterly wave, the monsoon trough, a surge in the monsoons, and cyclogenesis in the wave accumulation region.

Several researchers have noted that interactions of preexisting disturbances with upper-tropospheric troughs can lead to tropical cyclogenesis (Sadler 1976; Pfeffer and Challa 1981; Bosart and Bartlo 1991; Montgomery and Farrell 1993; Bracken and Bosart 2000. Briegel and Frank (1997) composited the flow in the western Pacific prior to genesis, and found that 85% of cases contained either an upper-tropospheric trough within 2500 km of the center or a lower-tropospheric wind surge. The wind surge typically took the form of an acceleration of the westerlies south of the monsoon trough before genesis. They attributed cyclogenesis in general to any forcing that can produce upward motion through a deep layer.

A number of researchers have noted the importance of interactions among mesoscale vortices during the cyclogenesis process (Ritchie and Holland 1993; Harr et al. 1996; Simpson et al. 1997). This mechanism cannot be addressed in the current paper because the ECMWF analyses cannot resolve such disturbances. Neverthe-

less, Simpson et al. (1997) noted that interacting mesoscale vortices are much more likely to lead to genesis when they occur within a larger-scale, lower-tropospheric, cyclonic circulation such as a monsoon trough.

Many of the above papers provide evidence for an enhancement of vorticity in the monsoon trough prior to tropical cyclogenesis in the western Pacific. It has been argued that the vast majority of western Pacific and Australian region tropical cyclones develop within the monsoon trough (Gray 1968; Zehr 1992; McBride and Keenan 1982). The role of easterly waves in these regions is less certain. Zehr's (1992) schematic and the work of Briegel and Frank (1997) and Sobel and Bretherton (1998) suggest that the interaction of easterly waves and the monsoon trough might represent an important cyclogenesis mechanism in the western Pacific.

b. Eastern Pacific cyclogenesis

The subtropical easterlies contain a diverse group of disturbances (Simpson et al. 1968; Wallace 1971; Krishnamurti et al. 1975; Wheeler and Kiladis 1999) that include equatorial Kelvin– and Rossby–gravity modes, surges in the trade winds, ITCZ or monsoon trough disturbances, easterly waves, and mesoscale convective complexes (Velasco and Fritsch 1987; Laing and Fritsch 1997). In addition, upper-tropospheric cold lows, both subtropical and extending from middle latitudes, produce extensive precipitation and interact with lower-tropospheric disturbances. The existence of this complex background complicates the study of tropical cyclogenesis.

Many theories have been put forth on the nature of tropical cyclogenesis in the eastern Pacific. Forecasters at the Tropical Prediction Center, who carefully track each wave and storm in real time, believe that virtually all eastern Pacific tropical cyclones develop in association with easterly waves that formed well upstream over Africa and propagated across the Atlantic and Central America and into the eastern Pacific (see, e.g., Avila and Pasch 1992). Shapiro (1986) showed specific examples of such propagation. Some previous operational forecasters (Simpson et al. 1968, 1969; Frank 1970) also associated genesis with waves in the easterlies but believed that roughly half of these waves developed outside of Africa, typically in the Caribbean. Bister and Emanuel (1997) studied the genesis of Hurricane Guillermo (1991) and found that it developed within a mesoscale convective system. They noted, however, that the genesis occurred in the presence of an easterly wave passing into the eastern Pacific. These papers place much greater importance on the easterly wave as the locus of tropical cyclone genesis than has been seen in the western Pacific.

Ferreira and Schubert (1997) have described a process whereby intertropical convergence zone (ITCZ) convection creates a low-level PV maximum and a sign reversal in the meridional PV gradient, followed by disturbance growth via the Charney–Stern instability theorem. Molinari et al. (1997) have described a correlation between the strength of such a PV gradient sign reversal in the Caribbean Sea and subsequent downstream cyclogenesis in the Pacific. Molinari et al. (1997) argued that African waves could be reinvigorated, or new waves could develop, on this unstable basic state. These waves would then be the locus of tropical cyclogenesis downstream. The low-pass PV gradient sign reversal variation followed that of low-pass filtered OLR, suggesting that the dynamically unstable basic state arose from the diabatic heating, as was proposed by Schubert et al. (1991) and Ferreira and Schubert (1997). Molinari et al. (1997) also noted the contribution of negative PV anomalies in the northern Caribbean in creating the sign reversal. These were attributed to the upward decrease of diabatic heating associated with surface sensible heat flux, shallow convection, and radiative cooling above the trade wind inversion. Molinari et al. (1997) argued that the dynamically unstable basic state provided a mechanism connecting the enhanced heating in the active phase of the MJO (or any other convective forcing) to enhanced tropical cyclogenesis.

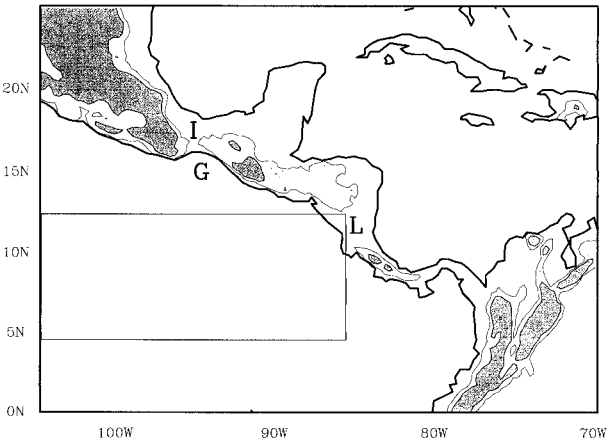

FIG. 1. Terrain height in the region of interest, averaged over 0.5° lat and long. Only two contours are shown: light shading is 500–1500 m; dark shading >1500 m. The letters refer to geographic regions discussed in the text: I, Isthmus of Tehuantepec; G, Gulf of Tehuantepec; L, the pass extending across Lake Nicaragua. The outlined rectangular area will be used for calculation of the mean values of 1000-mb wind speed (see section 4b).

The view of operational forecasters requires an easterly wave to enter the eastern Pacific from upstream, apparently from Africa. Ferreira and Schubert (1997) require no upstream wave but postulate the in situ breakdown of an unstable basic state forced by heating (the origin of the heating is left unstated). Molinari et al. (1997) observe an unstable basic state upstream and require an upstream wave, but not necessarily from Africa.

None of the above theories take any account of the substantial terrain that exists in Central and South America, shown in Fig. 1. This terrain is generally tall enough

to block or otherwise deflect the easterly flow that exists in the region in the lower troposphere (Mozer and Zehnder 1996; Farfan and Zehnder 1997). Mozer and Zehnder (1996) argued that broad easterly flow is blocked and diverted through the Isthmus of Tehuantepec (''I'' in Fig. 1). This leads to a barotropically unstable jet downstream and the continuous production of disturbances. No upstream wave was required for cyclogenesis in their hypothesis.

Farfan and Zehnder (1997) described and simulated the events leading to the genesis of Hurricane Guillermo in 1991. The circulation that became Guillermo first developed in the eastern Pacific while an easterly wave was in the Caribbean, upstream of the Central American mountains. The location and timing of the low-level prehurricane circulation were shaped by two low-level jets, an easterly jet through the opening in the mountains in the vicinity of Lake Nicaragua (''L'' in Fig. 1), and a northerly jet through the Isthmus of Tehuantepec. The latter flow occurred only in the moist simulation, for which the upstream wave amplitude remained large. Farfan and Zehnder (1997) thus required an upstream wave as part of the cyclogenesis process. But the predepression disturbance developed locally near the Gulf of Tehuantepec (''G'' in Fig. 1) rather than being associated directly with the passage of the original easterly wave into the eastern Pacific. The location and timing of tropical cyclogenesis appeared to be determined by mountain interactions, but in a more complex form than envisioned originally by the theory of Zehnder (1991).

The current work will attempt to evaluate the various ideas given above during the period before the formation of the pre–Hurricane Hernan depression on 0600 UTC 30 September 1996. It remains to be seen whether the conclusions of this study are valid for all or most eastern Pacific tropical cyclones. The following questions will be addressed for this cyclogenesis event:

1) Does the development of the pre–Hurricane Hernan depression occur in association with a synoptic-scale easterly wave? If so, does this wave come from upstream (east) of the Central American mountains, or even all the way from Africa?
2) Alternatively, does the depression development occur in situ with the monsoon trough without contribution from a preexisting disturbance from upstream?
3) What role do the Central American mountains play?
4) What role do local or upstream dynamical instabilities play in the development?

4. Results

a. Disturbances from Africa

Figure 2 shows a longitude–time (Hovmöller) plot of the bandpassed (2–6 day) v component of the wind at 700 mb. This is shown for 12.375°N during a 1-month period in September and October of 1996. Hovmöller diagrams at several adjacent latitudes, and for the 10.1°–14.6°N mean, are remarkably similar (not shown). Comparable plots at 900 mb (also not shown) look similar but with somewhat smaller amplitude. The hurricane symbols in Fig. 2 show the time and longitude at which tropical depressions within 4.5° lat of 12.375°N first appeared.

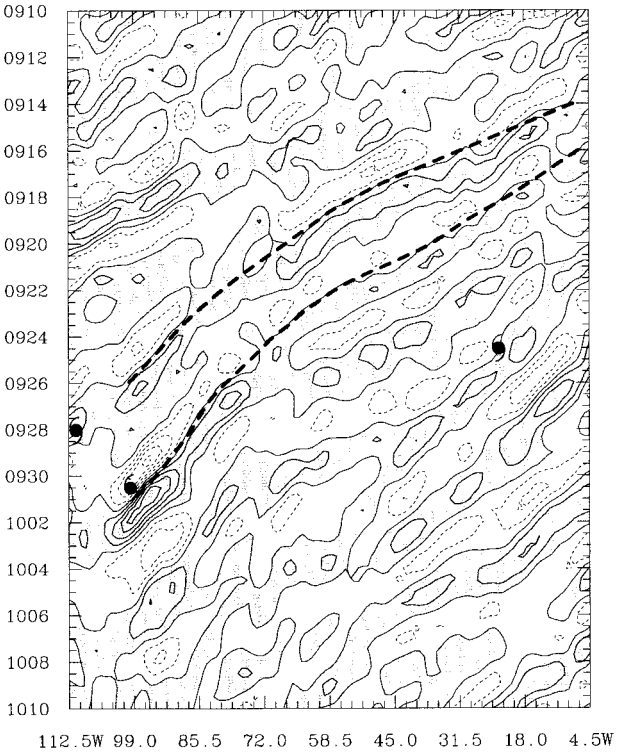

FIG. 2. Longitude–time section along 12.375°N at 700 mb of the bandpass-filtered (2–6 day) v component of the wind between 0000 UTC 10 Sep and 0000 UTC 10 Oct 1996. Positive values are shaded. The hurricane symbols mark the longitude and time of formation of tropical depressions within 4.5° lat of 12.375°N. The heavy dashed lines trace the axes of the two waves that excited eastern Pacific tropical cyclones during the period. Contour increment 1 m s^{-1}.

The 2–6-day period chosen for Fig. 2 corresponds well with the dominant mode found over Africa (Reed et al. 1977; Nitta and Takayabu 1985; Burpee 1974; Reed et al. 1988b; Lau and Lau 1990; Duvel 1990). The contribution of the 2–6-day mode to the total variance at each grid point at 700 mb was computed over the period 10 September–10 October 1996 (the same period as in the figure) using

$$\frac{\sum_{n=1}^{N} v^{*2}}{\sum_{n=1}^{N} (v - \overline{v})^2}, \tag{1}$$

where $N = 61$ (the number of 12-hourly analyses in the period), $\overline{v}$ is the time averaged v over the same period, and v^{*2} is the bandpass variance. It was found that the 2–6-day mode carried 40.9% of the total variance at

12.375°N, averaged over the longitudes shown in Fig. 2. It would appear, at least for this particular month, that easterly waves are a major contributor in the Atlantic basin.

The African coast at the latitude of Fig. 2 lies at 17°W. Waves in the easterlies in Fig. 2 can be tracked from Africa across the Atlantic and Caribbean and into the eastern Pacific. The axes of two such waves are marked in heavy dashed lines; each was associated with eastern Pacific depression formation: at 1800 UTC 27 September (which became Tropical Storm Genevieve); and at 0600 UTC 30 September (eventually Hurricane Hernan). The latter shows much more clearly than the former because Genevieve developed 450 km to the north of the latitude in Fig. 2. Both storms quickly moved northward and thus are seen only a short time in the figure. No other eastern Pacific storms occurred between 10 September and 6 November (L. Avila 1998, personal communication). Four other waves in Fig. 2 spawned Atlantic storms: Isidore (shown), Josephine (in the southwest Gulf of Mexico), and Kyle and Lilly (in the week just after the period shown in the figure).

The speed of motion of the waves associated with Genevieve and Hernan, calculated by connecting maxima in the time–longitude plot, was close to 11 m s^{-1} over the Atlantic, and 5 m s^{-1} in the Caribbean and eastern Pacific. These values are comparable to those determined by Reed et al. (1988a) for the two regions.

Figure 2 shows occasional large changes in the amplitude or phase speed of the disturbances. These arise when disturbances move meridionally away from the latitude of interest, and when upper-tropospheric troughs move southward into the region and induce southerlies over a wide area that are not directly associated with wave passage. The v component often decreases in magnitude at about 85°W, then increases again downstream. This is attributed to interaction with the higher terrain of Nicaragua at that latitude, as disturbances weaken by PV conservation reasoning as they move upslope.

Discontinuities can also arise as a result of weaknesses in the analysis. For instance, much of the tropical Atlantic contains only nonconventional data such as cloud-track winds. When waves in the model reach more data-rich regions in the Caribbean, there may be a mismatch in wave position and/or amplitude. Conventional rawinsonde data begin at about 60°W. Close examination of several Hovmöller diagrams including Fig. 2 does not indicate persistent discontinuities at this longitude (e.g., note the waves leading to Genevieve and Hernan). It is concluded that, although uncertainties exist in the analyses, the v component Hovmöller diagrams offer considerable support for an African origin for waves reaching the eastern Pacific Ocean during the period shown.

b. Genesis in the eastern Pacific

Figures 3a,b show low-pass filtered fields (20-day cutoff) at 700 and 1000 mb on 0000 UTC 28 September.

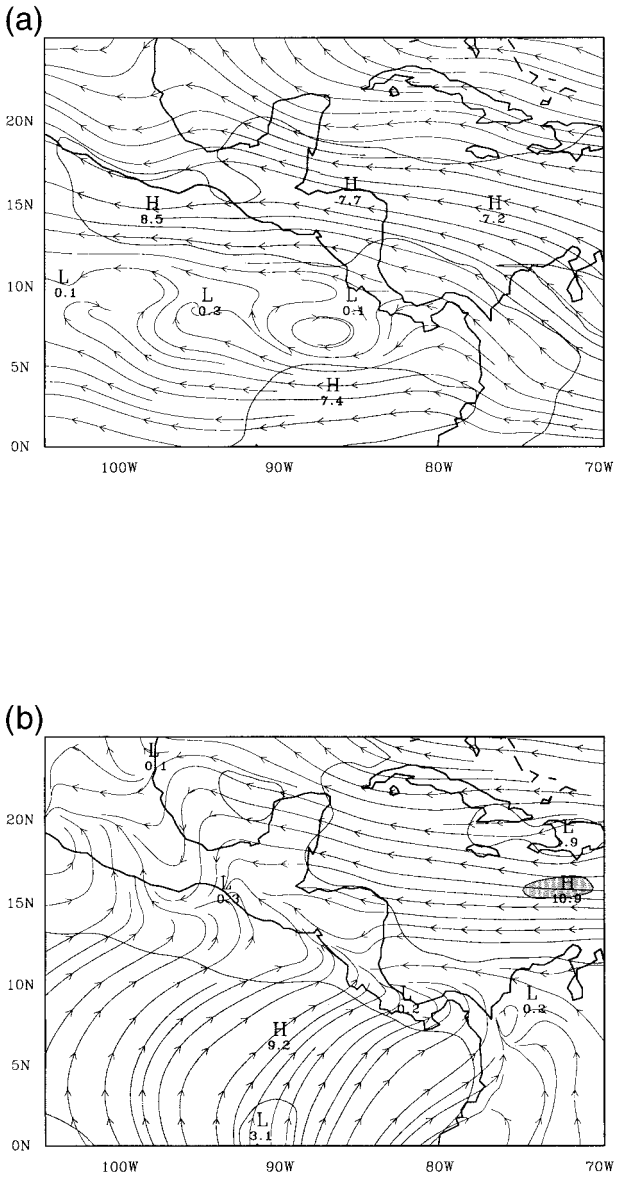

FIG. 3. Low-pass filtered (20-day cutoff) wind field for 0000 UTC 28 Sep 1996 at (a) 700 mb and (b) 1000 mb. These are interpreted as the background fields through which synoptic-scale disturbances pass. Light lines are streamlines; light and dark shading indicate wind speed 5–10 m s^{-1} and greater than 10 m s^{-1}, respectively.

The response function for this filter is shown by Molinari et al. (1997). Because by definition the low-pass filtered fields vary slowly, the time shown in Fig. 3 is representative of the entire 5-day period before development of the pre-Hernan depression. For the most part the Mexican and Central American terrain lies below 700 mb. The background flow shows broad easterlies with maximum speed at about 15°N. No indication of southwesterly monsoonal flow exists at 700 mb.

In land areas, much of the 1000-mb pressure surface lies below ground. The sophisticated ECMWF procedure for extrapolation to 1000 mb includes a planetary

boundary layer structure. Nevertheless, little meaning should be attached to the flow shown in Fig. 3b over high terrain; rather, the oceanic regions and the low-elevation mountain passes are of primary interest. The 1000-mb background flow shows broad trade wind easterlies east of the Central American mountains, and broad 5–10 m s^{-1} southwesterly monsoonal flow west of the mountains. A monsoon trough is far north during this time, essentially parallel to the south coast of Mexico. Weak northerly flow occurs through the Isthmus of Tehuantepec. Southwesterly monsoons exist at 925 mb as well, but are much weaker at 850 mb (not shown).

Recently Sobel and Bretherton (1998) showed that the region of confluence of the flow in the western Pacific where trade easterlies meet monsoon westerlies produces growth of Rossby waves of approximately 30% per day by a wave accumulation mechanism. In principle, the same could occur across Central America as easterly waves approach from the east, as is apparent from Fig. 3. But the waves tend to have largest amplitude at 700 mb, where the monsoon westerlies are absent. Only in the lower troposphere could such a mechanism occur, and even there it could be disrupted by mountain effects and large dissipation. The overall impact of the wave accumulation mechanism in the eastern Pacific is uncertain.

Figure 4 shows the low-pass filtered meridional gradient of absolute vorticity at 700 and 900 mb at 0000 UTC 28 September. Shaded regions in the figure indicate a northward decrease in absolute vorticity. At 700 mb, this background state satisfies the necessary condition for barotropic instability ($\partial\zeta_a/\partial y$ changing sign) in part of the Caribbean, and in an extended region near the Mexican coast in the eastern Pacific. At 900 mb, the sign reversal is even stronger and occurs over a wider area, especially in the Caribbean. Westward propagating waves at 10°–15°N during this period will thus be passing through a region in which the effective β is small or even of opposite sign to that of the earth. The lack of dispersion where $\partial\zeta_a/\partial y$ is small and the potential for barotropic instability each could contribute to maintenance or intensification of a disturbance.

Molinari et al. (1997) showed that the ITCZ is characterized by a localized PV (and also vorticity) maximum, with strong northward increase of absolute vorticity to the south, and a much weaker increase or even a decrease of absolute vorticity to the north. This structure is consistent with the idealized modeling of Schubert et al. (1991), and with the monsoon trough structure shown in Fig. 4b. The monsoon trough lies approximately along the equatorward edge of the shaded region near the southern Mexican coast (where $\partial\zeta_a/\partial y = 0$) at 1000 mb.

Figures 3–4 showed the low-pass filtered background through which disturbances in the easterlies travel. Figure 5 shows the evolution of the unfiltered 700-mb wind field once daily (at 0000 UTC) for 6 days, ending 18 h after the pre-Hernan tropical depression was declared.

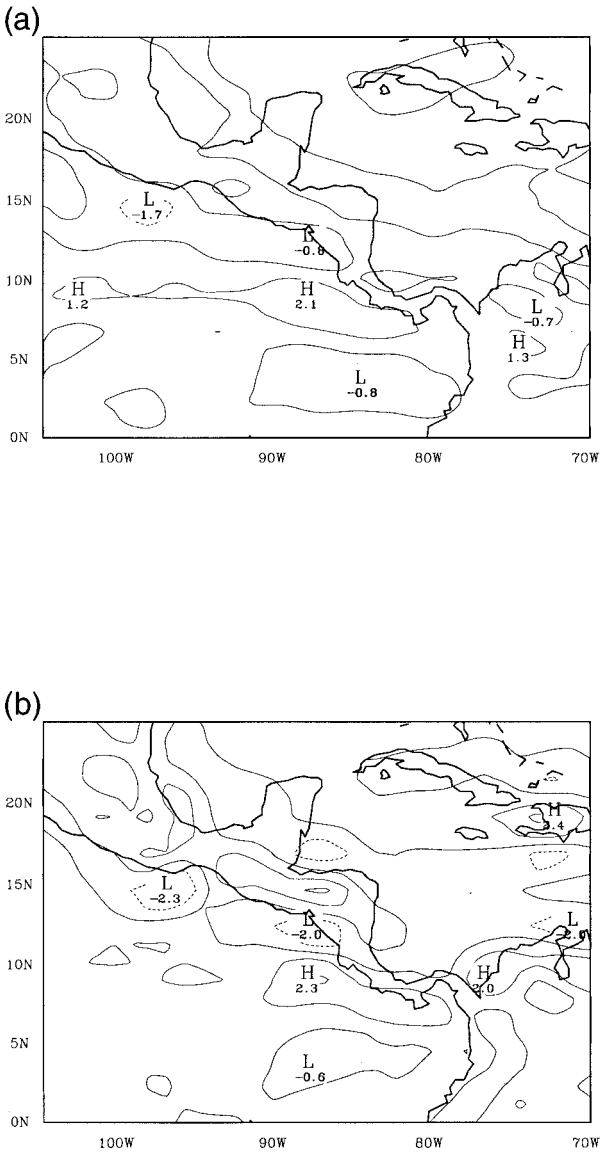

FIG. 4. Low-pass filtered meridional gradient of absolute vorticity at 0000 UTC 28 Sep 1996 at (a) 700 mb and (b) 900 mb. Shading indicates that $\partial\zeta_a/\partial y < 0$. Units: 10^{-11} s^{-1} m^{-1}.

The asterisk shows the center of circulation at 700 mb, and the × shows the center of circulation in the 2–6-day bandpass-filtered 700-mb wind. The two centers were virtually coincident throughout the period. Several characteristics of the synoptic-scale disturbance that eventually gave rise to Hurricane Hernan can be seen:

1) Although a closed circulation was present at 700 mb, the maximum wind remained north of the disturbance throughout the period.
2) The wind speed maximum in the disturbance intensified nearly 40% in 24 h (0000 UTC 26 September–0000 UTC 27 September) while it crossed the region

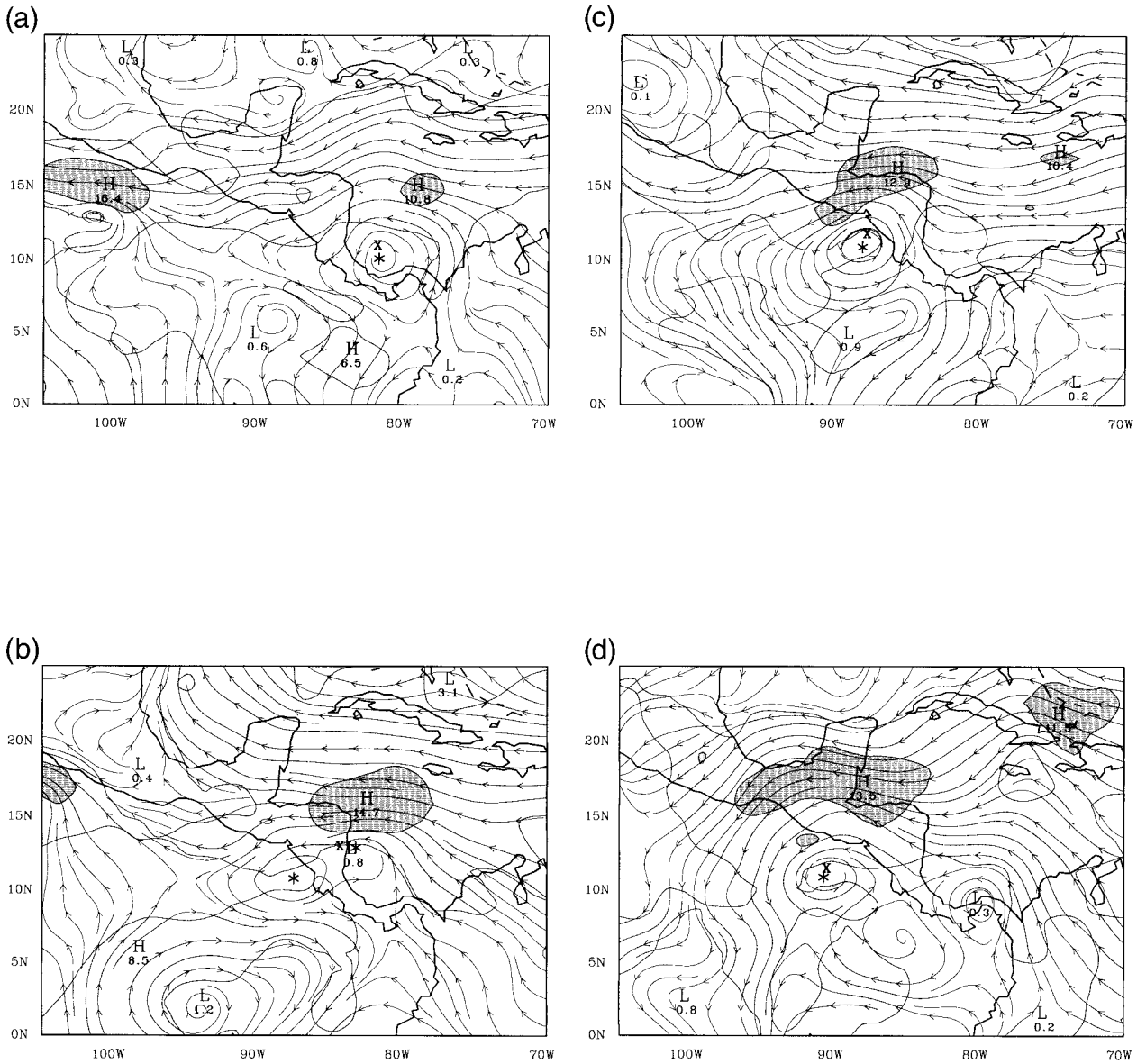

FIG. 5. Wind field at 700 mb every 24 h at 0000 UTC for (a) 26 Sep; (b) 27 Sep; (c) 28 Sep; (d) 29 Sep; (e) 30 Sep; (f) 1 Oct 1996. Streamlines and wind speed contours as in Fig. 3. The asterisk marks the center of circulation of the pre-Hernan disturbance in the easterlies. The × marks the center of circulation of the pre-Hernan disturbance at the same level, but from a bandpass-filtered (2–6 day) wind field.

of meridional absolute vorticity gradient sign reversal in the western Caribbean.

3) The center of circulation of the disturbance appeared influenced by the changes in terrain height underneath, in that it turned northward (anticyclonically) in the upslope region, then appeared at the original latitude on the other side of the Central American mountains. At 0000 UTC 27 September (Fig. 5b) circulations appeared on both sides of Central America, but a single disturbance appeared thereafter at the original latitude.
4) The disturbance progressed steadily westward through 0000 UTC 28 September, as did the jet north-northeast of the center. The strong northeasterly flow ahead of the wave axis reached the Isthmus of Tehuantepec at 0000 UTC 29 September (Fig. 5d).

Figure 6 shows the unfiltered 1000-mb wind field at the same times as Fig. 5. Also shown (asterisk) is the center of circulation at the 700-mb level. The structure varies quite dramatically from that at 700 mb:

1) When the 700-mb wave was east of the mountains a 1000-mb easterly jet accompanied the 700-mb wave, but about 200–300 km farther east. Once the 700-mb wave moved west of the mountains, no easterly wind maximum reappeared until the pre-Hernan

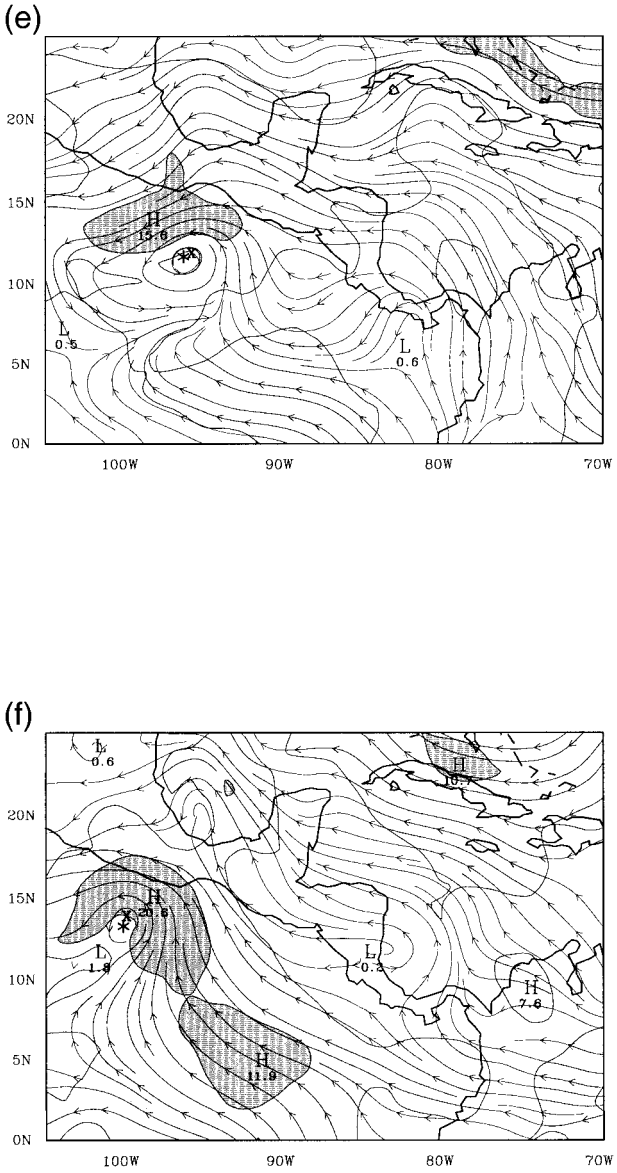

FIG. 5. (*Continued*)

depression was about to develop at 0000 UTC 30 September. Apparently the low-level easterly jet was blocked by the mountains. In the region of the wave axis the easterly flow at 1000 mb was above that of the background state (Fig. 3b).

2) Southwesterly monsoonal flow above that in the background state occurred at 1000 mb ahead of the 700-mb wave axis, and shifted westward with the wave. Unlike the case studied by Farfan and Zehnder (1997), easterly flow did not extend into the Pacific across the Lake Nicaragua latitude, apparently because the easterlies remained north of this latitude.
3) Northerly flow through the Isthmus of Tehuantepec began at 0000 UTC 29 September (Fig. 6d) as the 700-mb disturbance center came within 500 km of the Gulf of Tehuantepec.
4) After the 700-mb wave crossed the mountains and moved over water, a weak 1000-mb circulation appeared almost directly underneath it at 0000 UTC 28 September. This intensified into a strong circulation by 0000 UTC 30 September, and a tropical storm strength disturbance by 0000 UTC 1 October.

The time variation of 850–200-mb vertical wind shear centered on the center of circulation of the 700-mb disturbance was calculated following Molinari (1993). Values were remarkably similar whether 100, 300, or 500 km was chosen as the averaging radius. The vertical shear remained below 10 m s^{-1} until 28 September, when it rose to 10–12 m s^{-1} for 2 days, then fell back to 7 m s^{-1} on 0000 UTC 30 September. Examination of 850-mb and 200-mb maps (not shown) indicates that the lowered shear arose because cross-storm flow at 200 mb vanished on the 30 September as outflow from the center became much more pronounced. The evidence suggests that weaker shear followed development of the surface vortex and of strong convection (see Fig. 8 for the latter) rather than preceding it.

A possible key factor in development is given in Fig. 7, which shows relative vorticity at 1000 mb during a time of rapid deepening at 1200 UTC 29 September (halfway between the times of Figs. 6d and 6e). A well-defined vorticity maximum is present at about 11.9°N, 93.8°W associated with the merging of the original disturbance under the 700-mb wave (Fig. 5d) and the cyclonic half of a strong vorticity dipole associated with flow through the Isthmus of Tehuantepec. These features were separate 12 h earlier (not shown). In addition, enhanced vorticity occurs west of the 700-mb wave axis along 10°–12°N, associated with the surge in the monsoons. This provides a more favorable environment for development (e.g., McBride 1995) in the region toward which the disturbance is moving.

Although it cannot be said with certainty due to the 12-h separation of the analyses, the evidence from Fig. 7 suggests that the 1000-mb spinup of vorticity during 29 September might relate in part to an acceleration of flow through the opening in the mountains at the Gulf of Tehuantepec. This process was noted by Farfan and Zehnder (1997) to play an important role in the numerical simulation of the genesis of Hurricane Guillermo of 1991. In the current study it appears that 700-mb wave moved over the quasi-stationary region of large surface vorticity associated with flow through the Isthmus, and the resultant vertical coupling acted to enhance the surface disturbance.

A considerable effort was made to confirm the strong flow through the Isthmus of Tehuantepec shown in the ECMWF analyses. Unfortunately, the surface stations located in the Isthmus often did not report. Those that did report were sheltered by higher terrain around the Isthmus. This problem has been remedied, at least tem-

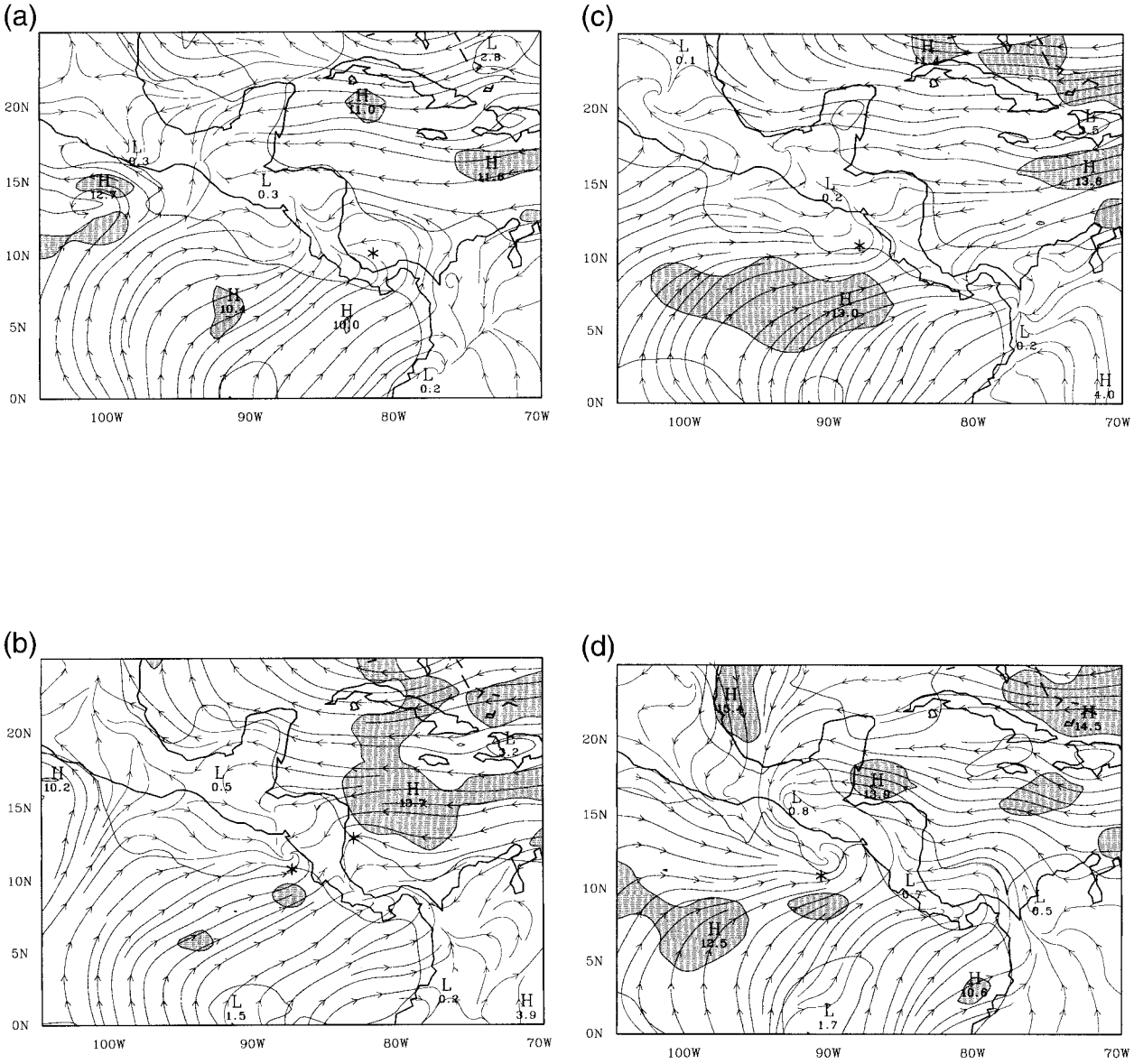

FIG. 6. As in Fig. 5 but for the 1000-mb level. The asterisk indicates the location of the center of the 700-mb circulation.

porarily, by Pan American Climate Studies stations, but these did not begin operating until 1997. The strong flow through Tehuantepec, and its role in cyclogenesis, must remain a hypothesis based on the gridded analyses rather than a certainty.

Instead, gridded OLR data were used to provide an independent evaluation of the evolution indicated by the ECMWF analyses. The OLR data were filtered to keep only 2-day and longer periods. This was done because the enormous diurnal oscillation of convection in the region (M. Douglas 1998, personal communication) can mask the wave signature.

Figure 8 shows once daily OLR at five observation times beginning on 26 September. Only OLR values less than or equal to 180 W m^{-2} are shown; this contour corresponds best with the areal coverage of deep convection on satellite images. The heavy dashed line in Fig. 8 connects the center of circulation at 700 mb with the point of maximum wind in the jet to the north at each observation time (see Fig. 5). This gives a measure of the meridional tilt of the wave. Figure 8 shows that the convective maximum associated with the wave moves from along and east of the 700-mb wave axis in the Caribbean to west of the wave axis in the Pacific. Enhanced OLR, and thus enhanced convection, also occurs along 10°N well ahead of the 700-mb wave axis except for one period (0000 UTC 27 September; Fig. 8b) when the wave is interacting with the mountains. At the final time (0000 UTC 30 August; Fig. 8e), a strong localized maximum in OLR (101 W m^{-2}) has

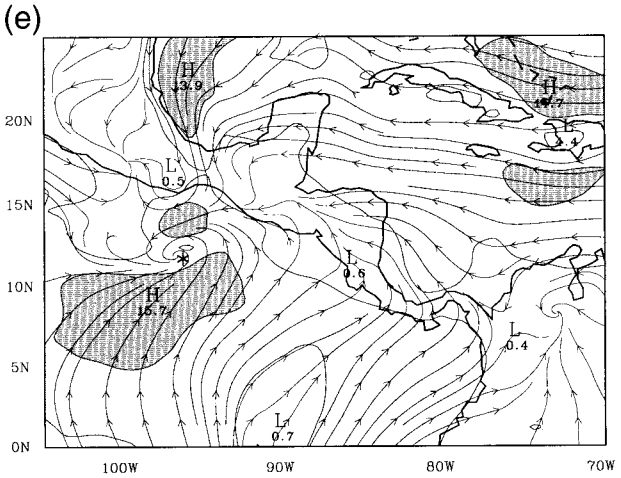

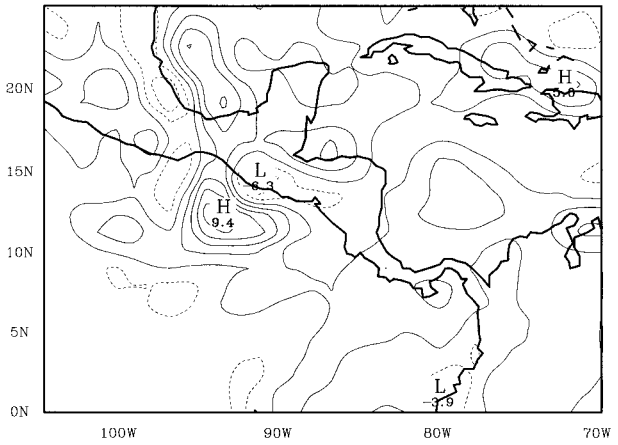

FIG. 7. Unfiltered relative vorticity at 1000 mb at 1200 UTC 29 Sep as the pre-Hernan surface circulation intensified. The contour increment is 2×10^{-5} s^{-1}. Positive values are shaded.

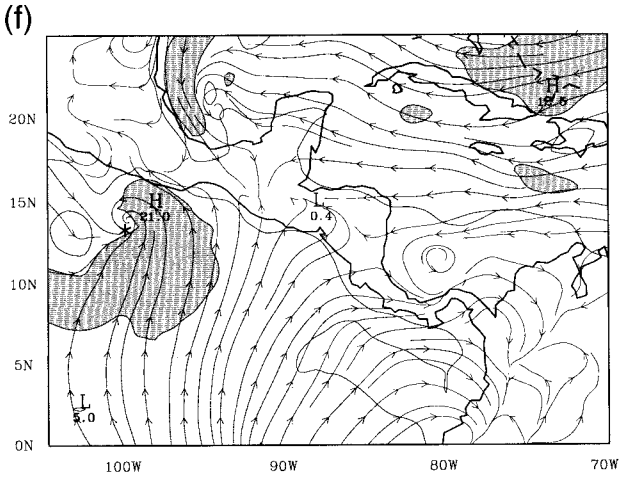

FIG. 6. (*Continued*)

developed near the center of the developing low-level disturbance shown in Figs. 5e and 6e. This is interpreted as the beginning of the shift from wave characteristics to depression characteristics in both the wind and OLR fields. The areal coverage of deep convection grew considerably at the same time, extending northward along the vorticity dipole in the Isthmus of Tehuantepec, again consistent with the gridded analyses (Figs. 6d,e and 7). The tilt of the wave remained southwest–northeast throughout, until the final time when growth of the localized disturbance makes the tilt less meaningful.

The increased convective activity along 10°N ahead of the 700-mb wave axis (Fig. 8) is consistent with the stronger southwesterly monsoons at 1000 mb south of the monsoon trough (Fig. 6). The stronger monsoonal flow produces stronger vorticity in the monsoon trough and thus the likelihood of stronger convection. As noted earlier, Zehr (1992) produced a schematic diagram of western Pacific cyclogenesis in which a surge in the monsoons occurs west-southwest of a wave in the easterlies. The evolution shown in the ECMWF analyses, and the corroboration of that evolution in the OLR data, suggests that the development of the pre-Hernan depression in the eastern Pacific has some aspects in common with cyclogenesis in the western Pacific. The surge appears to be directly linked to the 700-mb wave rather than being an independent phenomenon. A wind maximum from the northeast at 200 mb (not shown) also tracks westward ahead of the 700-mb wave and almost exactly opposes the low-level surge. The depth of this divergent circulation supports the conclusion from the OLR data that convection is playing a major role in the surge.

Figure 9 provides an indication of the relationship between synoptic-scale waves, OLR, and surges in the monsoons over the 1-month period. The wind surge is difficult to define in terms of the u or v components of the wind separately. Rather, increase of the southerlies at 1000 mb is often followed by increase in the westerlies (one-quarter of the inertial period is about 17.5 h at 10°N). The surge will be defined in terms of the mean wind speed rather than either wind component. A region is chosen (see the box in Fig. 1) that brackets the increase in the southwest monsoons shown in Fig. 6. Figure 9 shows the mean wind speed over this box. In addition, Fig. 9 shows mean 1000-mb vorticity and mean OLR for a box with the same east–west boundaries, but shifted northward by approximately 5° lat from the wind box. For consistency with the OLR data, both winds and vorticity have also been filtered to remove periods less than 2 days.

Figure 9 shows evidence in the 1000-mb vorticity

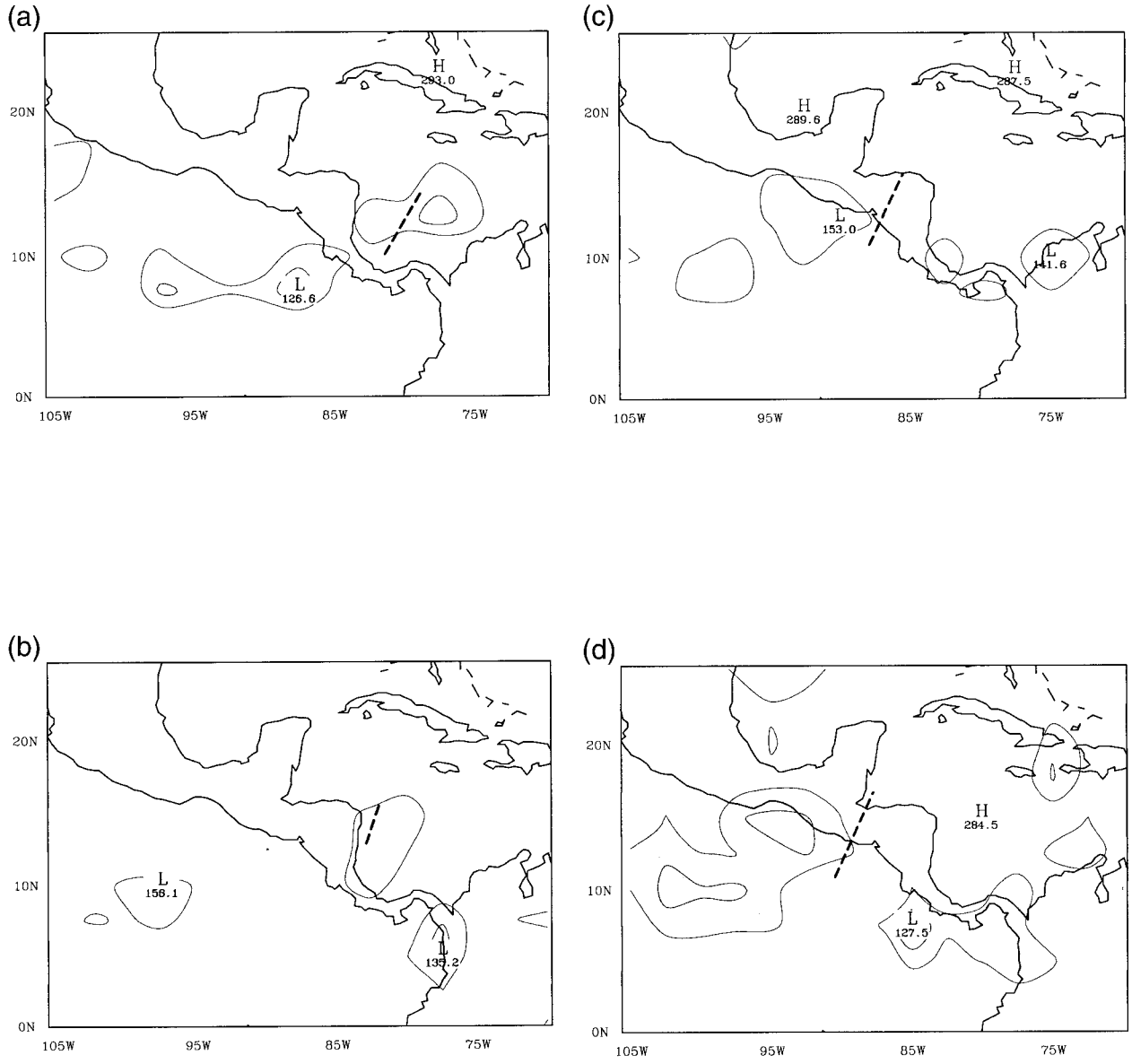

FIG. 8. Outgoing longwave radiation (OLR), filtered to remove periods of less than 2 days. Only the contours less than or equal to 180 W m^{-2} are shown, representing the locations of active deep convection. Contour increment: 30 W m^{-2}. The heavy dashed line connects the center of circulation at 700 mb with the point of maximum wind speed in the jet north of the disturbance (see Fig. 5), and represents a measure of the meridional tilt of the wave.

of five 700-mb wave passages, labeled W1–W5. Accompanying each wave, a maximum appears in surface wind speed and in convective activity as measured by OLR. From middle to late September, an apparent longer period oscillation occurs, as mean vorticity remains cyclonic and both mean wind and mean OLR increase for about 2 weeks, but the wave scale still shows well on top of this longer period oscillation. The latter may simply relate to the presence of tropical cyclones Genevieve and Hernan within the box and the associated increases in mean wind speed and convection.

5. Discussion

The four questions from the end of section 3 will be addressed first. The pre-Hernan depression does indeed occur in association with a synoptic-scale wave in the easterlies, rather than having an in situ origin in the eastern Pacific monsoon trough. The wave, identified by the 2–6-day mode in the meridional component of the wind, can be tracked back to Africa. Several other waves during the month were of African origin, including the wave associated with Tropical Storm Genevieve in the eastern Pacific.

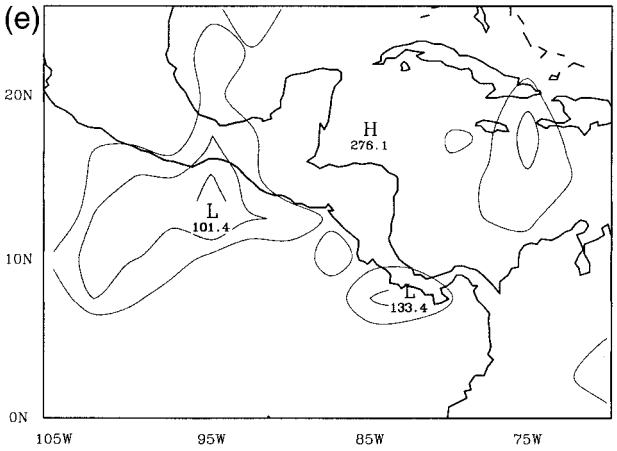

FIG. 8. (*Continued*)

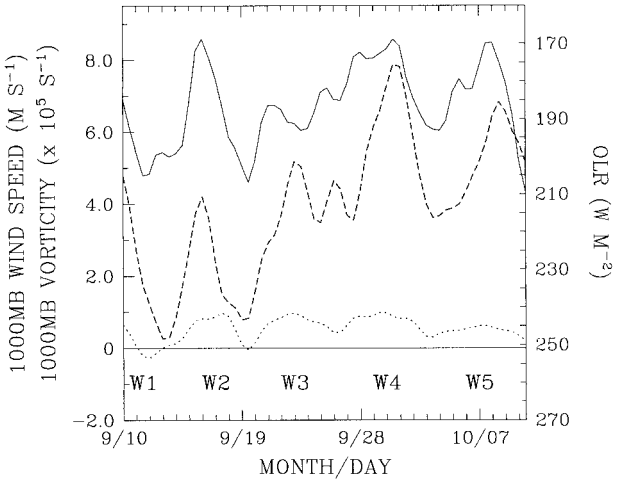

FIG. 9. Evolution of mean 1000-mb wind speed (m s^{-1}; solid) over the box shown in Fig. 1. Also shown are mean 1000-mb vorticity ($\times 10^5$ s^{-1}; dotted) and mean OLR (W m^{-2}; dashed) for the same size box, but shifted 5° lat northward. To be consistent with the OLR data, both wind and vorticity are filtered to keep periods 2 days or greater. The Ws represent the 1000-mb reflections of 700-mb wave passages through the box.

The Central American mountains also played a role in cyclogenesis. In Farfan and Zehnder's (1997) study the synoptic-scale wave apparently remained northeast of the mountains, and the disturbance west of the mountains grew initially at the surface as a result of flow through passes, then built upward from the surface. In the present study, the pre-Hernan depression developed underneath the 700-mb wave after the latter moved across the mountains and into the Pacific. Turk et al. (1995) found two types of storm tracks in the region: in the first, waves tracked north and east of the Central American mountains, followed by a secondary development south of the Gulf of Tehuantepec. In the second storm track, waves crossed Central America near Lake Nicaragua and continued westward across the eastern Pacific, and genesis occurred directly with the primary wave. It appears that the case of Farfan and Zehnder (1997) resembles the first track, while the current case resembles the second.

Enhanced low-level flow from the north through the Isthmus of Tehuantepec ahead of the 700-mb wave axis shows clearly in the analyses, but could not be confirmed or refuted by available data. It is hypothesized that such flow creates cyclonic vorticity at the surface that vertically couples with the 700-mb wave as the latter moves westward. The enhanced northerly flow may simply represent a response to falling surface pressure south of the isthmus underneath the mobile 700-mb wave. Once the 700-mb circulation extends to the surface in this fashion, depression development is much more likely as the system continues to move westward. This speculation cannot be confirmed by the twice daily analyses, but some indirect evidence exists to support such a conclusion. First, Laing and Fritsch (1997) show a maximum in mesoscale convective complex occurrence at and just west of the Gulf of Tehuantepec in summer and fall. Second, Fig. 10 shows a plot of the number of tropical depression formations from 1949 to 1996 as a function of longitude in the eastern Pacific. By far the strongest increase in depression formation occurs at the Gulf of Tehuantepec and points west.

Finally, the background state showed a sign reversal in the meridional gradient of absolute vorticity in the Caribbean and especially the eastern Pacific. In the study by Molinari et al. (1997), it was the fluctuation of the Caribbean and eastern Pacific sign reversals that cor-

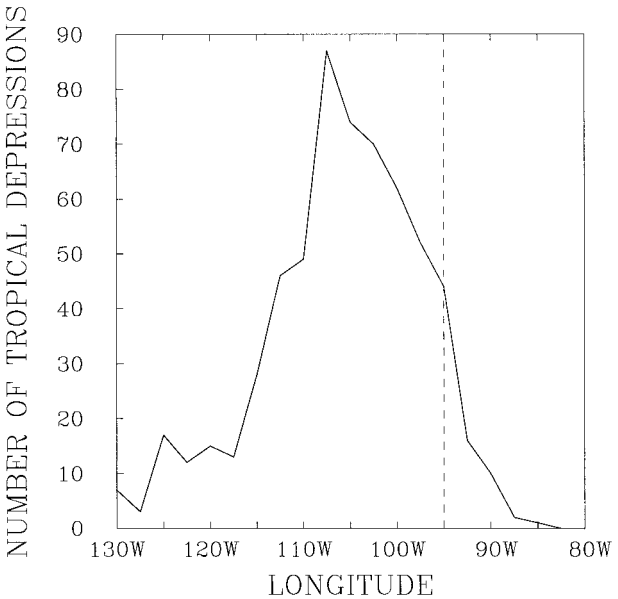

FIG. 10. Longitudinal variation of the frequency of formation of tropical depressions in the eastern Pacific from 1949 to 1996. All such depressions south of 22.5°N are included. The dashed line indicates the longitude of the Gulf of Tehuantepec (source: National Hurricane Center ''best track'' dataset).

related with subsequent eastern Pacific cyclogenesis. In this study the background state vorticity gradients did not have large-amplitude fluctuations, but the sign reversal remained strong during the period of interest. The wave clearly moved through an unstable basic state as it intensified in the western Caribbean and eastern Pacific.

The unstable background state cannot be proven to be a key component without idealized numerical experiments. But there are two ways in which it can contribute to development. Most obviously, it encourages growth of the disturbance. But there also exists a lengthy region where $\partial\zeta_a/\partial y$ is near zero in the Caribbean and eastern Pacific. In this region a disturbance in the easterlies will avoid loss of amplitude by dispersion. Lau and Lau (1990) calculated disturbance growth rates in the region. Growth occurred primarily in locations of sign reversal of the meridional gradient of PV (Molinari et al. 1997) or absolute vorticity (Fig. 4 of this paper), including 75°–80°W and 90°–110°W. Those calculations support the contribution of the sign reversal to wave growth.

The development of the pre-Hernan depression described above appears to contain components of several theories of eastern Pacific cyclogenesis: a preexisting easterly wave from Africa; mountain interaction; a dynamically unstable background state; and a surge in the monsoons. But the evidence suggests that wave passages control events, including surges in the monsoons. It is proposed that if a strong wave crosses the mountains and SSTs are favorable (almost always true in summer and early fall) and vertical wind shear is small (which it is climatologically; Gray 1979), that cyclogenesis is likely. By this reasoning it is the strength of the waves reaching Central America that determines the likelihood of eastern Pacific cyclogenesis. This conclusion is based on a single case study during a month that waves were unusually active, and thus remains speculative. But it is consistent with the results of Farfan and Zehnder (1997), who showed that strong northerly flow through the Isthmus of Tehuantepec associated with cyclogenesis occurred only when the upstream wave maintained a large amplitude.

In the western Pacific some of the same factors are present as in this case study, particularly the presence of easterlies meeting monsoon westerlies and a monsoon trough. It is proposed that to the extent easterly waves are active upstream of the monsoon trough, such waves might organize wind surges and cyclogenesis in the western Pacific as well.

Acknowledgments. The ECMWF gridded analyses were obtained from the National Center for Atmopheric Research, which is supported by the National Science Foundation. The outgoing longwave radiation data of Liebmann and Smith (1996) were obtained electronically; we thank Catherine Smith of the University of Colorado for her assistance in this process. Positions of eastern Pacific tropical cyclones were obtained electronically from the National Hurricane Center (NHC). We thank Lixion Avila and Richard Pasch of NHC for providing additional information on Hurricane Hernan and on easterly waves and tropical cyclones during the 1996 season. This work is supported by National Science Foundation Grant ATM-9529771 and Office of Naval Research Grant N00014-98-10599.

REFERENCES

Avila, L. A., and R. J. Pasch, 1992: Atlantic tropical systems of 1991. *Mon. Wea. Rev.,* **120,** 2688–2696.

Bister, M., and K. A. Emanuel, 1997: The genesis of Hurricane Guillermo: TEXMEX analyses and a modeling study. *Mon. Wea. Rev.,* **125,** 2662–2682.

Bosart, L. F., and J. A. Bartlo, 1991: Tropical storm formation in a baroclinic environment. *Mon. Wea. Rev.,* **119,** 1979–2013.

Bracken, W. E., and L. F. Bosart, 2000: The role of synoptic-scale flow during tropical cyclogenesis over the North Atlantic Ocean. *Mon. Wea. Rev.,* in press.

Briegel, L. M., and W. M. Frank, 1997: Large-scale influences on tropical cyclogenesis in the western North Pacific. *Mon. Wea. Rev.,* **125,** 1397–1413.

Burpee, R. W., 1974: Characteristics of the North African easterly waves during the summers of 1968 and 1969. *J. Atmos. Sci.,* **31,** 1556–1570.

Charney, J. G., and A. Eliassen, 1964: On the growth of the hurricane depression. *J. Atmos. Sci.,* **21,** 68–75.

Davidson, N. E., and H. H. Hendon, 1989: Downstream development in the Southern Hemisphere monsoon during FGGE/WMONEX. *Mon. Wea. Rev.,* **117,** 1458–1470.

Duvel, J. P., 1990: Convection over tropical Africa and the Atlantic Ocean during northern summer. Part II: Modulation by easterly waves. *Mon. Wea. Rev.,* **118,** 1855–1868.

Emanuel, K. A., 1986: An air–sea interaction theory for tropical cyclones. Part I: Steady-state maintenance. *J. Atmos. Sci.,* **43,** 585–604.

——, J. D. Neelin, and C. S. Bretherton, 1994: On large-scale circulations in convecting atmospheres. *Quart. J. Roy. Meteor. Soc.,* **120,** 1111–1144.

Farfan, L. M., and J. A. Zehnder, 1997: Orographic influence on the synoptic-scale circulations associated with the genesis of Hurricane Guillermo (1991). *Mon. Wea. Rev.,* **125,** 2683–2698.

Ferreira, R. N., and W. H. Schubert, 1997: Barotropic aspects of ITCZ breakdown. *J. Atmos. Sci.,* **54,** 261–285.

Frank, N. L., 1970: Atlantic tropical systems of 1969. *Mon. Wea. Rev.,* **98,** 307–314.

Frank, W. M., 1987: Tropical cyclone formation. *A Global View of Tropical Cyclones,* R. L. Elsberry, Ed., Naval Postgraduate School, 53–90.

Gray, W. M., 1968: Global view of the origin of tropical disturbances and storms. *Mon. Wea. Rev.,* **96,** 669–700.

——, 1979: Hurricanes: Their formation, structure, and likely role in the tropical circulation. *Meteorology over the Tropical Oceans,* D. B. Shaw, Ed., Royal Meteorology Society, 155–218.

Gruber, A., and J. S. Winston, 1978: Earth–atmosphere radiative heating based on NOAA scanning radiometer measurements. *Bull. Amer. Meteor. Soc.,* **59,** 1570–1573.

Harr, P. A., R. L. Elsberry, and J. C. L. Chan, 1996: Transformation of a large monsoon depression to a tropical storm during TCM-93. *Mon. Wea. Rev.,* **124,** 2625–2643.

Holland, G. J., 1995: Scale interaction in the western Pacific monsoon. *Meteor. Atmos. Phys.,* **56,** 57–79.

Krishnamurti, T. N., C. E. Levy, and H.-L. Pan, 1975: On simultaneous surges in the trades. *J. Atmos. Sci.,* **32,** 2367–2370.

Laing, A. G., and J. M. Fritsch, 1997: The global population of

mesoscale convective complexes. *Quart. J. Roy. Meteor. Soc.*, **123,** 389–406.
Lau, K.-H., and N.-C. Lau, 1990: Observed structure and propagation characteristics of tropical summertime synoptic scale disturbances. *Mon. Wea. Rev.,* **118,** 1888–1913.
Liebmann, B., and H. H. Hendon, 1990: Synoptic-scale disturbances near the equator. *J. Atmos. Sci.,* **47,** 1463–1479.
——, and C. A. Smith, 1996: Description of a complete (interpolated) outgoing longwave radiation dataset. *Bull. Amer. Meteor. Soc.*, **77,** 1275–1277.
——, H. H. Hendon, and J. D. Glick, 1994: The relationship between tropical cyclones of the western Pacific and Indian Oceans and the Madden–Julian oscillation. *J. Meteor. Soc. Japan,* **72,** 401–411.
Lorenc, A. C., 1981: A global three-dimensional multivariate statistical interpolation scheme. *Mon. Wea. Rev.,* **109,** 701–721.
Love, G., 1985: Cross-equatorial influence of winter hemisphere subtropical cold surges. *Mon. Wea. Rev.,* **113,** 1487–1498.
Madden, R. A., and P. R. Julian, 1994: Observations of the 40–50-day tropical oscillation—A review. *Mon. Wea. Rev.,* **122,** 814–837.
McBride, J. L., 1995: Global perspectives on tropical cyclones. World Meteorological Organization Report No. TCP-38, 289 pp.
——, and R. Zehr, 1981: Observational analysis of tropical cyclone formation. Part II: Comparison of non-developing versus developing systems. *J. Atmos. Sci.,* **38,** 1132–1151.
——, and T. D. Keenan, 1982: Climatology of tropical cyclone genesis in the Australian region. *J. Climatol.,* **2,** 13–33.
Merrill, R. T., 1984: A comparison of large and small tropical cyclones. *Mon. Wea. Rev.,* **112,** 1408–1418.
Molinari, J., 1993: Environmental controls on eye wall cycles and intensity change in Hurricane Allen (1980). *Tropical Cyclone Disasters,* J. Lighthill et al., Eds., Peking University Press, 328–337.
——, and D. Vollaro, 1990: External influences on hurricane intensity. Part II: Vertical structure and response of the hurricane vortex. *J. Atmos. Sci.,* **47,** 1902–1918.
——, ——, and F. Robasky, 1992: Use of ECMWF operational analyses for studies of the tropical cyclone environment. *Meteor. Atmos. Phys.,* **47,** 127–144.
——, S. Skubis, and D. Vollaro, 1995: External influences on hurricane intensity. Part III: Potential vorticity structure. *J. Atmos. Sci.,* **52,** 3593–3606.
——, D. Knight, M. Dickinson, D. Vollaro, and S. Skubis, 1997: Potential vorticity, easterly waves, and tropical cyclogenesis. *Mon. Wea. Rev.,* **125,** 2699–2708.
Montgomery, M. T., and B. F. Farrell, 1993: Tropical cyclone formation. *J. Atmos. Sci.,* **50,** 285–310.
Mozer, J. B., and J. A. Zehnder, 1996: Lee vorticity production by large-scale tropical mountain ranges. Part I: Eastern North Pacific tropical cyclogenesis. *J. Atmos. Sci.,* **53,** 521–538.
Nitta, T., and Y. Takayabu, 1985: Global analysis of the lower tropospheric disturbances in the Tropics during the northern summer of the FGGE year. Part II: Regional characteristics of the disturbances. *Pure Appl. Geophys.,* **123,** 272–292.
Ooyama, K. V., 1964: A dynamical model for the study of tropical cyclone development. *Geophys. Int.,* **4,** 187–198.
——, 1982: Conceptual evolution of the theory and modeling of the tropical cyclone. *J. Meteor. Soc. Japan,* **60,** 369–379.
Pfeffer, R. L., and M. Challa, 1981: A numerical study of the role of eddy fluxes of momentum in the development of Atlantic hurricanes. *J. Atmos. Sci.,* **38,** 2393–2398.
Reed, R. J., D. C. Norquist, and E. E. Recker, 1977: The structure and properties of African wave disturbances as observed during Phase III of GATE. *Mon. Wea. Rev.,* **105,** 317–333.
——, A. Hollingsworth, W. A. Heckley, and F. Delsol, 1988a: An evaluation of the performance of the ECMWF operational system in analyzing and forecasting easterly wave disturbances over Africa and the tropical Atlantic. *Mon. Wea. Rev.,* **116,** 824–865.
——, E. Klinker, and A. Hollingsworth, 1988b: The structure and characteristics of African easterly wave disturbances as determined from the ECMWF operational analysis/forecast system. *Meteor. Atmos. Phys.,* **38,** 22–33.
Riehl, H., 1954: *Tropical Meteorology.* McGraw-Hill, 392 pp.
Ritchie, E. R., and G. J. Holland, 1993: On the interaction of tropical-cyclone-scale vortices. Part I: Observations. *Quart. J. Roy. Meteor. Soc.,* **119,** 1363–1380.
Sadler, J. C., 1976: A role of the tropical upper tropospheric trough in early season typhoon development. *Mon. Wea. Rev.,* **104,** 1266–1278.
Schubert, W. H., P. E. Ciesielski, D. E. Stevens, and H. Kuo, 1991: Potential vorticity modeling of the ITCZ and the Hadley circulation. *J. Atmos. Sci.,* **48,** 1493–1509.
Shapiro, L. J., 1986: The three-dimensional structure of synoptic-scale disturbances over the tropical Atlantic. *Mon. Wea. Rev.,* **114,** 1876–1891.
Simpson, J., E. Ritchie, G. J. Holland, J. Halverson, and S. Stewart, 1997: Mesoscale interactions in tropical cyclone genesis. *Mon. Wea. Rev.,* **125,** 2643–2661.
Simpson, R. H., N. Frank, D. Shideler, and H. M. Johnson, 1968: Atlantic tropical disturbances, 1967. *Mon. Wea. Rev.,* **96,** 251–259.
——, ——, ——, and ——, 1969: Atlantic tropical disturbances of 1968. *Mon. Wea. Rev.,* **97,** 240–255.
Smith, R. K., 1997: On the theory of CISK. *Quart. J. Roy. Meteor. Soc.,* **123,** 407–418.
Sobel, A. H., and C. S. Bretherton, 1998: Development of synoptic-scale disturbances over the summertime tropical northwest Pacific. *J. Atmos. Sci.,* **56,** 3106–3127.
Turk, M., D. Vollaro, and J. Molinari, 1995: Large-scale aspects of active and inactive periods of eastern Pacific tropical cyclogenesis. Preprints, *21st Conf. on Hurricanes and Tropical Meteorology,* Miami, FL, Amer. Meteor. Soc., 106–107.
Velasco, I., and J. M. Fritsch, 1987: Mesoscale convective complexes in the Americas. *J. Geophys. Res.,* **92,** 9591–9613.
Wallace, J. M., 1971: Spectral studies of tropospheric wave disturbances in the tropical western Pacific. *Rev. Geophys. Space Phys.,* **9,** 557–611.
Wheeler, M., and G. N. Kiladis, 1999: Convectively coupled equatorial waves: Analysis of clouds and temperature in the wavenumber–frequency domain. *J. Atmos. Sci.,* **56,** 374–399.
Zehnder, J. A., 1991: The interaction of planetary-scale tropical easterly waves with topography: A mechanism for the initiation of tropical cyclones. *J. Atmos. Sci.,* **48,** 1217–1230.
Zehr, R. M., 1992: Tropical cyclogenesis in the western North Pacific. NOAA Tech. Rep. NESDIS 61, 181 pp. [Available from National Technical Information Service, Sills Building, 5285 Port Royal Rd., Springfield, VA 22161.]